Supporting Information

A Bird Nest-Inspired and Fully Biomass Coating with an Interpenetrating Fibrous Network for Thermal Insulation and Universal Fire Retardancy

Xue Gou[1], Ting Wang[1, 2] *, Yong-Qi Liang[1], Jiajiamo Luo[1], Chengxu Xu[1], Jinni Deng[1, 2], Zhi-Cheng Fu[1, 2], Wenli An[1, 2], Ming-Jun Chen[1, 2] *

1 Green Preparation and Recycling Laboratory of Functional Polymeric Materials, College of Science, Xihua University, Chengdu, Sichuan, 610039, China

2 Sichuan Engineering Research Center for Molecular Targeted Diagnostic & Therapeutic Drugs

* Corresponding author:

E-mail: wanting_nina@163.com (Ting Wang); cmjchem@126.com (Ming-Jun Chen)

Supplementary Figure

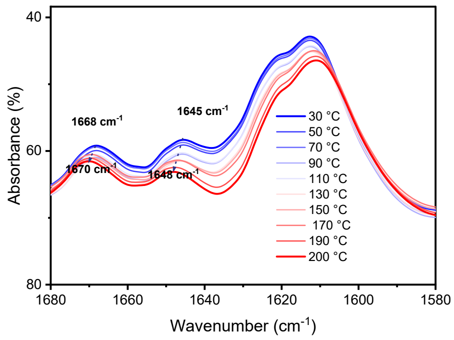

Fig. S1. FTIR spectra of C2G4 coating from 30 ℃ to 200 °C.

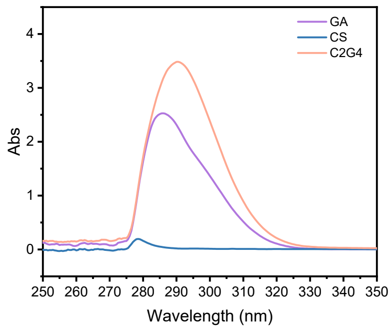

Fig. S2. UV-vis spectra of GA, CS, and C2G4.

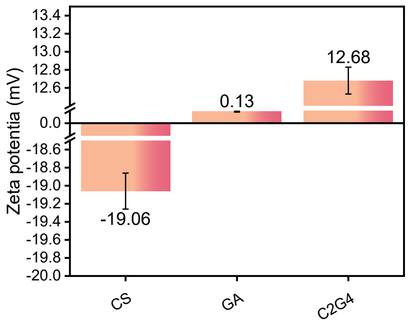

Fig. S3. Zeta potential values of GA, CS, and C2G4 solutions.

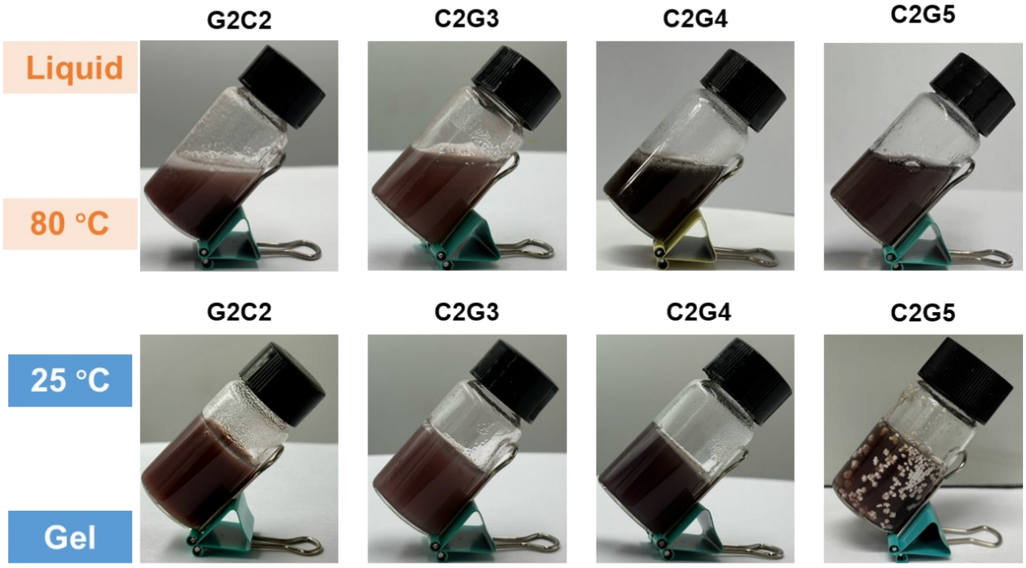

Fig. S4. Images of C2G2, C2G3, C2G4, and C2G5 at 80 °C and room temperature.

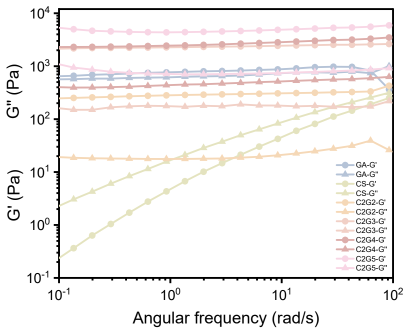

Fig. S5. Rheological properties of CG gel.

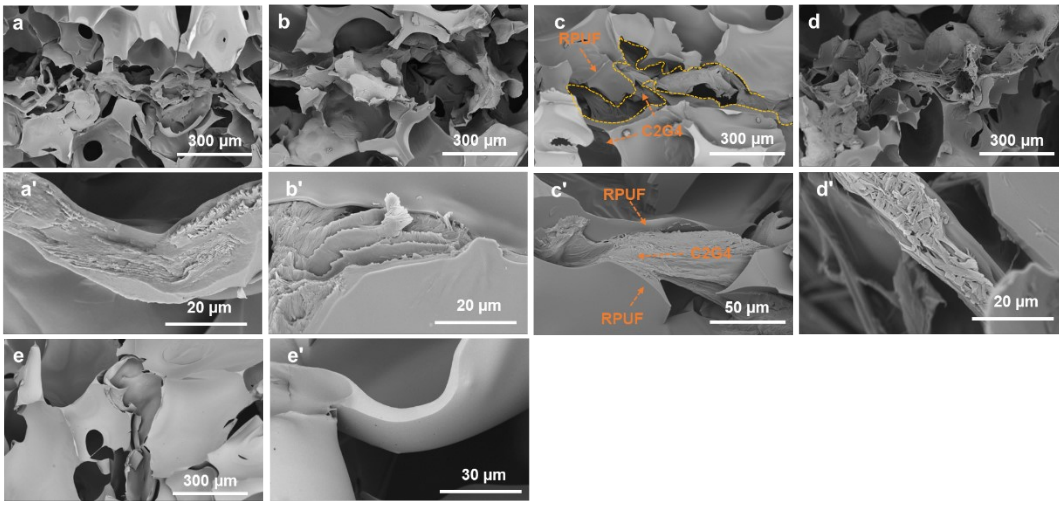

Fig. S6. SEM images of CG adhered to RPUF. (a)C2G2@RPUF, (b) C2G3@RPUF, (c) C2G4@RPUF, (d) C2G5@RPUF, (e) CS@RPUF.

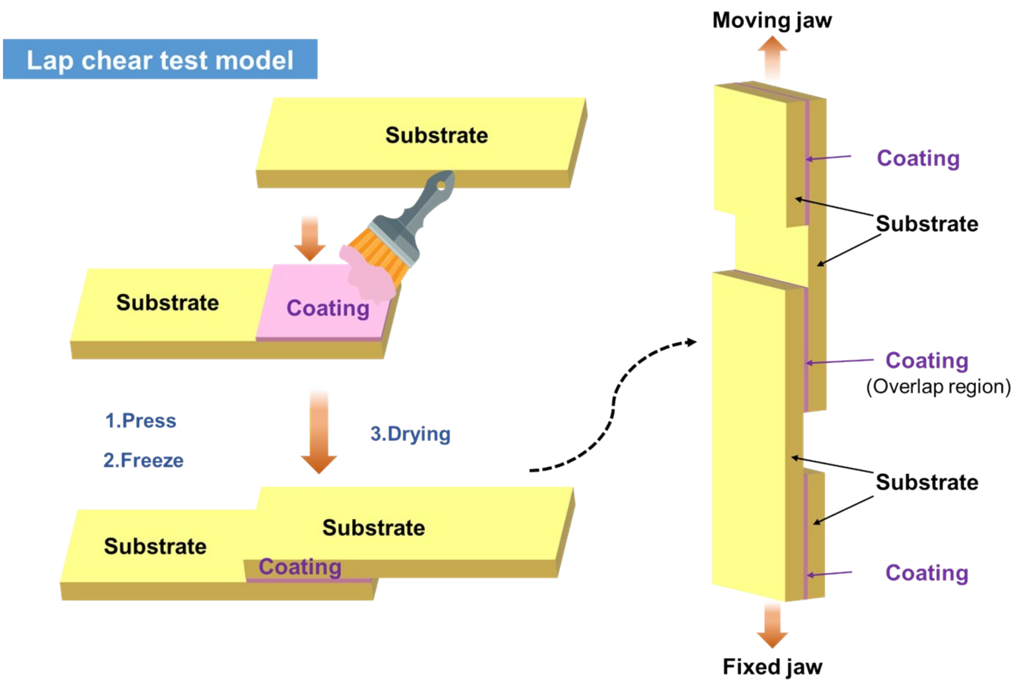

Fig. S7. Lap shear test model.

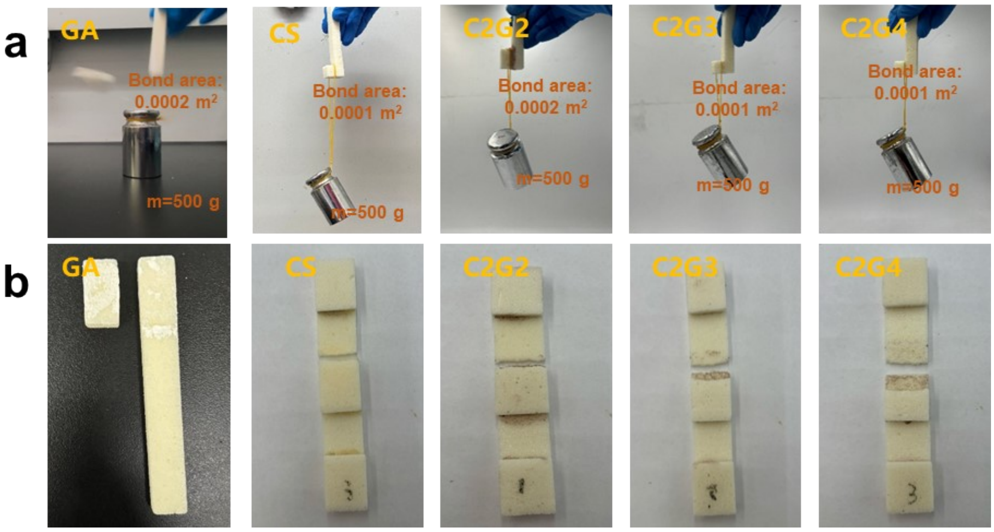

Fig. S8. Images of CG adhered to RPUF. (a) Digital photograph of a 500 g weight lapped on CG@RPUF. (b) Digital photograph of CG@RPUF after testing with a universal testing machine.

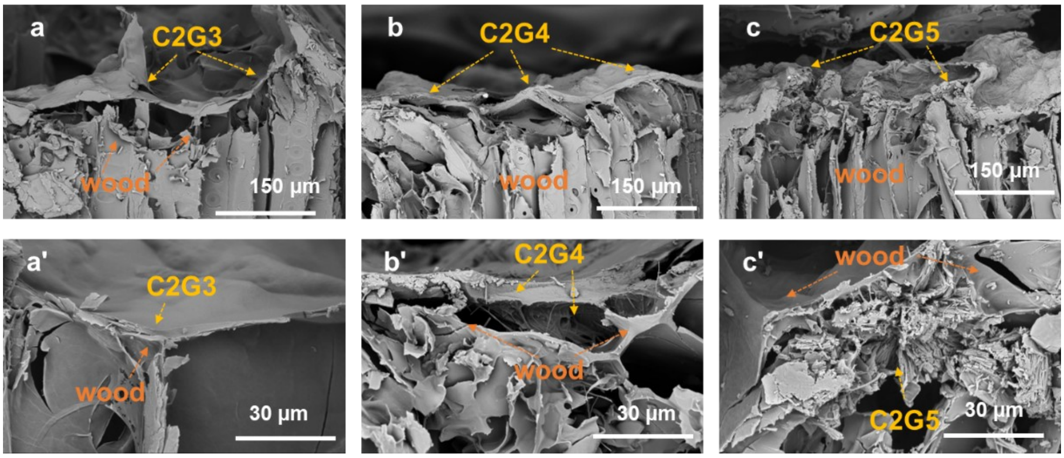

Fig. S9. SEM images of CG coatings with different ratios showing their microstructures: (a) C2G3@RPUF, (b) C2G4@RPUF, (c) C2G5@RPUF

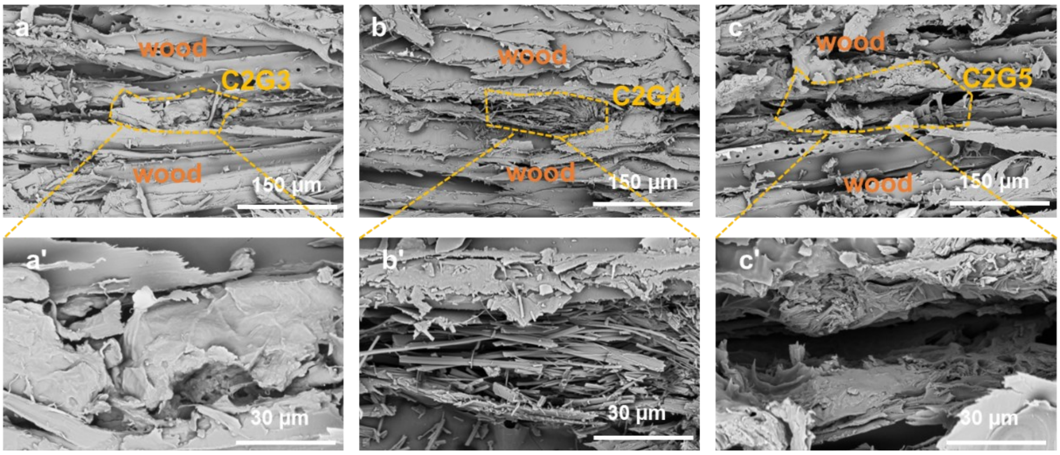

Fig. S10. Cross-sectional SEM images of CG adhered to wood. (a) C2G3@ wood, (b) C2G4@ wood, (c) C2G5@ wood.

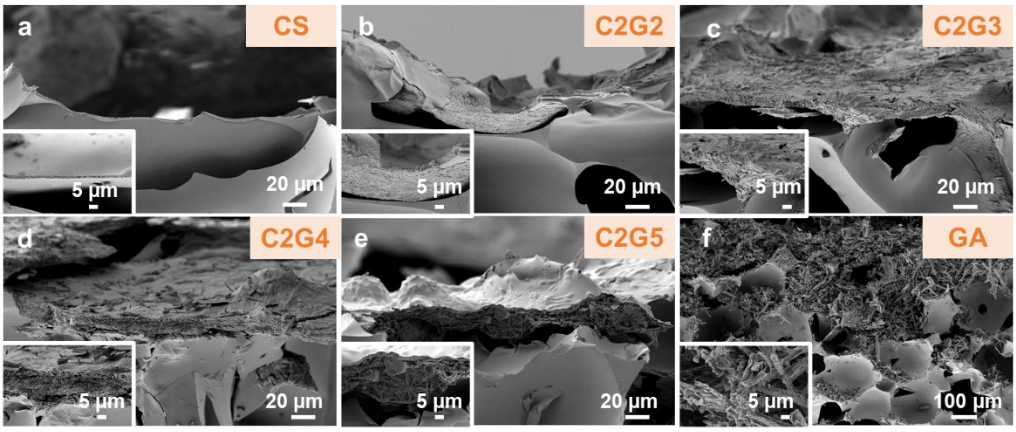

Fig. S11. SEM images of CG coatings with different ratios showing their microstructures: (a) CS@RPUF, (b) C2G2@RPUF, (c) C2G3@RPUF, (d) C2G4@RPUF, (e) C2G5@RPUF, (f) GA@RPUF.

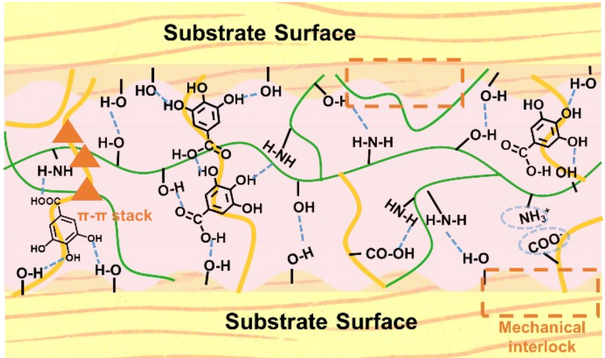

Fig. S12. Schematic diagram of C2G4 bonding on the substrate.

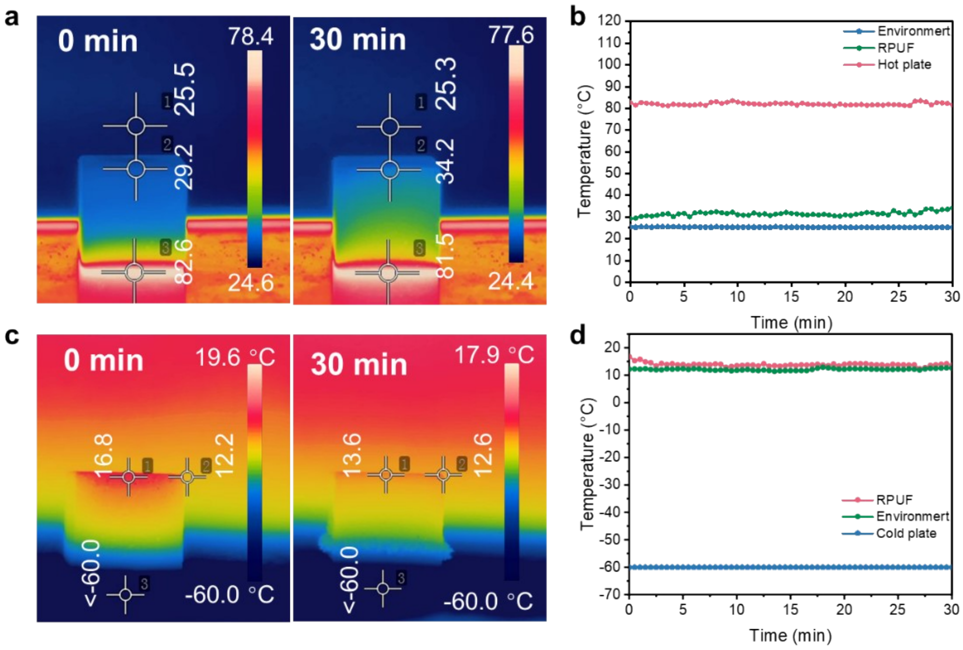

Fig. S13. Infrared thermal imaging monitoring photos and time-dependent temperature curves of RPUF on hot stage and cold stage. (a) Pseudo-color thermal image of the RPUF composite on the hot plate. (b) Temperature curve of RPUF on the hot plate as a function of time. (c) Pseudo-color thermal image of RPUF on the cold plate. (d) Temperature curve of the composite on the cold plate as a function of time.

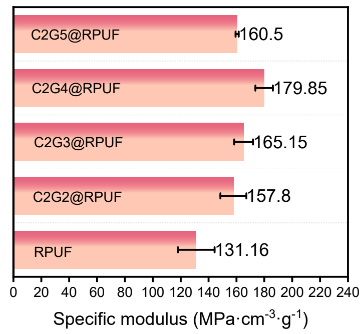

Fig. S14. Specific modulus of pure RPUF and coated RPUF.

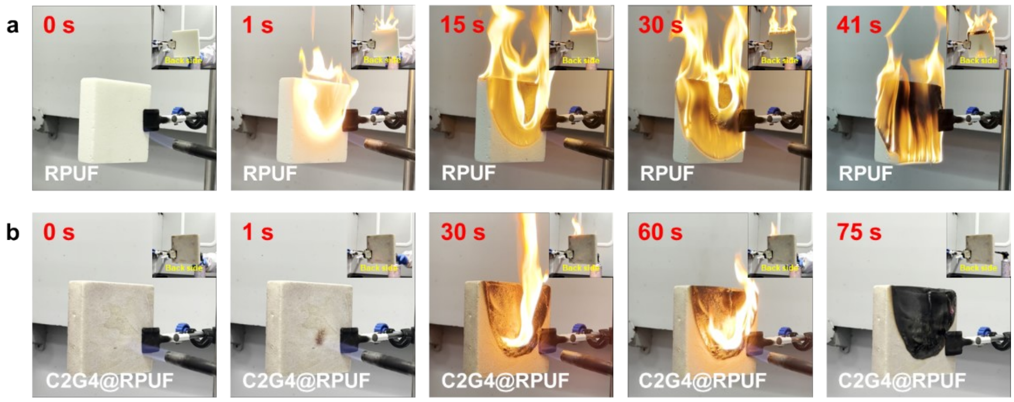

Fig. S15. Digital photographs of (a) RPUF and (b) C2G4@RPUF after butane burning at 1200 °C.

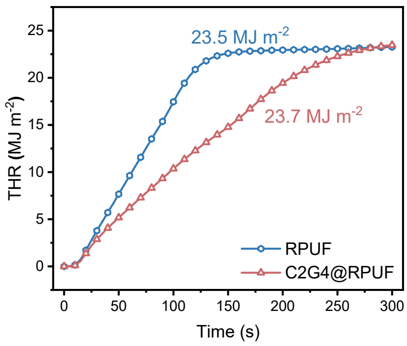

Fig. S16. THR curves of RPUF and C2G4@RPUF

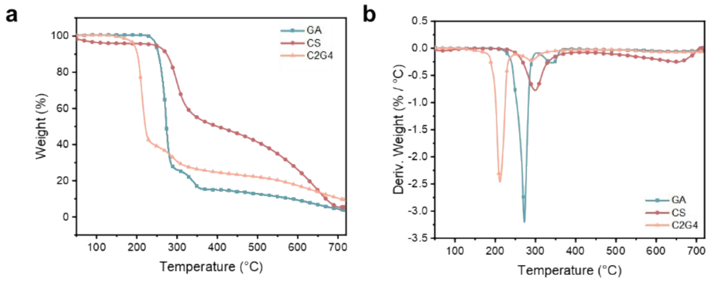

Fig. S17. TGA and DTG curves of GA, CS, and C2G4 under nitrogen atmosphere.

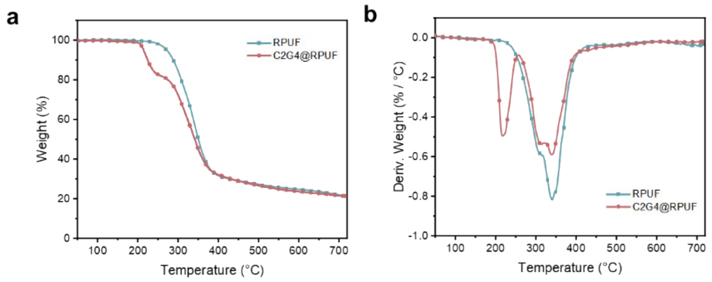

Fig. S18. TGA and DTG curves of pure RPUF and C2G4@RPUF under nitrogen atmosphere.

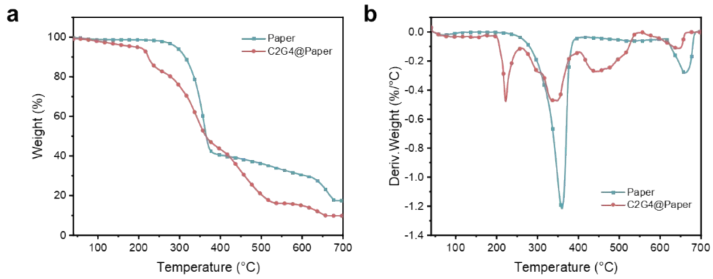

Fig. S19. TGA and DTG curves of pure Paper and C2G4@Paper under nitrogen atmosphere.

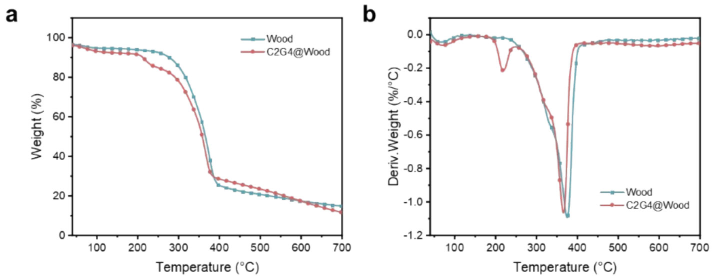

Fig. S20. TGA and DTG Curves of pure Wood and C2G4@Wood under nitrogen atmosphere.

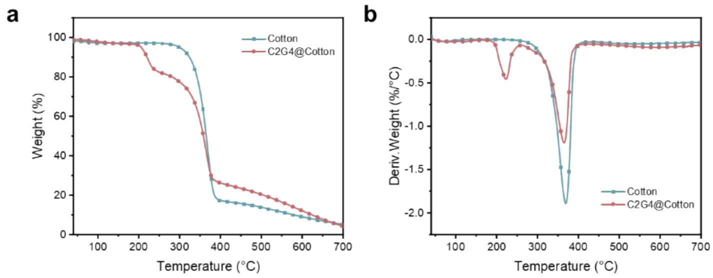

Fig. S21. TGA and DTG curves of pure Cotton and C2G4@Cotton under nitrogen atmosphere.

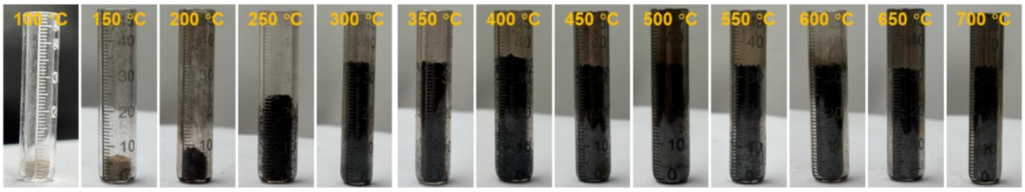

Fig. S22. States of C2G4 Heated at Different Temperatures in a Quartz Tube.

Supplementary Tables

Tab. S1. Formulations of pure RPUF.

Samples	**4110 (php[a])**	**A-1 (php)**	**T_{12} (php)**	**AK8805 (php)**	**H_2O (php)**	**C_5H_{12} (php)**	**PMDI (php)**
RPUF	100.0	0.2	0.16	2.5	1.0	5.0	131.4

(a) php: parts per hundred polyether polyols by weight.

Tab. S2. Weight gain rate of C_2G_4 on different substrates

Samples	RPUF	Paper	Wood	Cotton
Weight gain rate （wt %）	15±0.5	18±0.5	8±0.5	22±0.5

Tab. S3. Thickness of CG coating, compressive strength, compressive modulus, and thermal conductivity of pure RPUF and coated RPUF.

Samples	**Thickness (μm)**	**Density（mg cm^{-3}）**	**Compressive strength (Mpa)**	**Compressive modulus (Mpa)**	**Specific modulus (Mpa cm^{-3} g^{-1})**	**Thermal conductivity (mW m^{-1} K^{-1})**
RPUF	0	53.87±0.38	0.53±0.080	7.07±0.67	131.16±13.18	28.33±0.36
C2G2@RPUF	5.45±0.5	55.67±3.61	0.62±0.002	8.75±0.05	157.8±9.35	27.63±0.67
C2G3@RPUF	11.49±5.42	52.29±1.04	0.57±0.036	8.63±0.27	165.15±6.76	27.38±0.13
C2G4@RPUF	17.45±4.51	52.07±1.17	0.59±0.032	9.37±0.43	179.85±6.25	24.85±0.35
C2G5@RPUF	26.71±15.22	53.27±0.12	0.59±0.008	8.55±0.05	160.5±1.12	25.06±0.23

Tab. S4. Detailed data for pure GA, CS, C2G4, RPUF, C2G4@RPUF, Paper, C2G4@Paper, Wood, C2G4@Wood, Cotton, and C2G4@Cotton were obtained from TGA measurements at a heating rate of 10 °C/min over a temperature range from 50 °C to 720 °C.

Samples	$T_{5\%}$[a] (°C)	$T_{50\%}$[a] (°C)	T_{max1}[a] (°C)	T_{max2}[a] (°C)	T_{max3}[a] (°C)	T_{max4}[a] (°C)	Residue $Char_{700\,°C}$[b] (wt %)
GA	247	273	272	341	-	-	4.5
CS	243	400	299	644	-	-	5.5
C2G4	193	221	211	290	-	-	10.3
RPUF	272	350	340	-	-	-	21.9
C2G4@RPUF	214	341	217	313	338	-	21.6
Paper	291	365	359	659	-	-	17.5
C2G4@Paper	195	364	222	348	442	644	9.9
Wood	89	365	375	-	-	-	14.8
C2G4@Wood	66	357	70	218	365	-	11.6
Cotton	277	361	364	-	-	-	11.0
C2G4@Cotton	205	358	222	365	-	-	4.3

(a) $T_{5\,\%}$, $T_{50\,\%}$, T_{max1}, T_{max2}, T_{max3}, and T_{max4} refer to the temperatures at which 10 % weight loss, 50 % weight loss, and the first, second, third, and fourth maximum weight losses occur, respectively.
(b) Residues at 700 °C

Tab. S5. Cone calorimeter testing data for RPUF and C2G4@RPUF.

Spmples	Pure RPUF	C2G4@RPUF
pHRR[a] (kW m^{-2})	219.0±6.57	175.8±16.5
AHRR[a] (kW m-[2])	79.5±0.5	70.8±0.93
pSPR[b] (m^2 s^{-1})	0.067±0.010	0.042±0.005
TSP[b] (m^2)	5.5±0.37	3.9±0.17
Initial Mass (g)	14.4±0.7	17.8±0.5
Mass loss (g)	12.0±0.4	12.6±0.6
Mass loss (wt%)	83.2±2.57	70.6±0.5
pCOP[b] (mg s^{-1})	0.0039±0.0002	0.00250±0001
pCOY[b] (kg kg^{-1})	4.56±0.25	0.62±0.02
FGI[c] (kW m^{-1} s^{-1})	13.4±0.68	10.1±0.78
FPI[c] (m^2 s kW^{-1})	0.018±0.003	0.023±0.001

(a) pHRR and AHRR refer to peak heat release rate and average heat release rate, respectively.

(b) pSPR, TSP, pCOP, and pCOY refer to peak smoke production rate, total smoke production, peak carbon monoxide production rate, and peak carbon monoxide release rate, respectively.

(c) FPI and FGI refer to fire performance index and fire growth index, respectively.

Tab. S6 Other published bio-based flame-retardant RPUF composites

Method	FRs	P content （wt %）	LOI (%)	Δ pHRR (%)	Δ TSP (%)	Thermal conductivity (mW/(m K))	Δ Compressive strength (%)	Flame-retardant elements	Refs.
Coating	**C2G4@RPUF**	**0**	**29**	**-19.7**	**-29.1**	**24.8 (-12.3%)**	**+10.37**	**C/O/N**	**This work**
	Coated RPUF-4	3.87	39.7	-60.1	-20.6	-	-	C/O/N/P	Yu et al.[1]
	RPUF3/APP@PDA/PEI/PDA@ODT	-	42.5	-20.3	-14.01	40.7 (+0.7)	-	C/O/N/P/S	Han et al.[2]
	RPUF/$H_{pH=2}$-PEC	15.98	28.0	-41	-16.1	27.5 (-8.3)	+17.0	C/O/N/P	Luo et al.[3]
	CS/GEL/PA-Na	2.9	-	-53.5	-	-	-	C/O/N/P	Tang et al.[4]
	G5A3@RPUF	11.98	31	-49.4	-24.7	24.0(-14.3%)	37.5%	C/O/N/P	Feng et al.[5]
	CS-BP/PUF	-	26.3	-39.5	+53.7	-	-0.3	C/O/N/P	Yin et al.[6]
	RPUF/PAC_3	-	28.2	-61.8	-88.8	-	+3.4	C/N/O/P	Fang et al.[7]
	RPU/P1B7M2	6.28	24.8	-0.3	+40.1	34.4 (-0.2)	+4.6	C/O/N/P	Yang et al.[8]
	RPUF-10A/3S	14.31	60	-53.52	+116.5	28.1 (-15.1)	-	C/N/O/P/Si	Gao et al.[9]
	Ct-RPUF/L/FR	1.59	25.3	-8.6	-24.9	30.11 (-8.79)	+22.0	C/O/N/P/Si	Li et al.[10]
Additive	RPUF/L/FR	1.72 w	24.0	-45.29	-7.9	33.01(+11.5)	+10.42	C/N/O/P	Li et al.[10]
	CA/OSEP12.5	-	24.1	-52.1	-18.7	-	+35.3	C/O/N/Si/P/Mg	Zhang et al.[11]
	CP3	0	23.1	-55.5	-78	-	+65	C/O/N/S/Si/Al	Su et al.[12]
	RPUF-C3	0.85	22.1	-19.0	-4.4	-	+14.9	C/O/N/P	Zhang et al.[13]
	C/N-RPUF/5 wt% DOPOP	0.58	26.5	-39.6	-78.4	51.0 (+7.8)	+36.2	C/O/N/P	Selvaraj et al.[14]
	RPUF3	0.08	19.7	-29.7	-0.2	40.4 (+3.6)	+51.8	C/O/N/P	Han et al.[2]
	RPUF-C5ST2SE3	0	23.4	-35.9	-18.19	-	+19.9	C/O/Si/Mg/N	Zhang et al.[15]
Reactive	L3PU-G3	1.77	31.8	-61.9	-29.4	50 (-25%)	+540%	C/O/N/P	Sun et al.[16]
	RPUFc-150	0	18	-	-	34.2 (-5.5)	-6.2	C/O/N/S	Fidan et al.[17]
	1.6Hex-TEP	17	21.8	+9.2	-12.0	26.02 (+2.0)	-5.9	C/O/P	Zemła et al.[18]
	BIO2/EG/GO	2.4	27.2	-54.4	-15.5	34.2 (-31.0)	+57.1	C/O/N/P	Acuña et al.[19]
	F_REF	0	19.9	-	-	23.7 (-5.2)	-22.5	C/O	Hoyos-Martinez et al.[20]
Reactive and Additive	7B-PU/5SiO_2/ATH_{250}	0	24	-41.7	+6.6	46.0 (+21.1)	-1.4	C/N/O/Si/Al	Nguyen-Ha et al.[21]
	RPUF-D10	-	-	-	-	-	-34.16	C/O/P/Al	Zhang et al.[22]
	dPUF/10E/10D	2.22	25.7	0	+61.7	30.9 (+7.6)	-23.8	C/O/P	Akdogan et al.[23]
	RPUF/15VED/15EG	1.1	30.5	-66.1	-63	35 (+16.7)	+16.9	C/O/N/P	Chen et al.[24]
	RPUF/7.5%LP-2.5%EG	0.78	25.6	-28.2	-21.9	-	+39.6	C/O/N/P/Si	Cao et al.[25]
Packing	G5PA0.5/RPUF	1.91	28.5	-38	-54	28.6 (-21.6)	+93.69	C/O/N/P	Yu et al.[26]

References

1 J. K. Yu, L. Sun, L. Ding, Y. F. Cao, X. H. Liu, Y. L. Ren and Y. S. Li, *Polym. Degrad. Stabil.*, 2024, **227**, 110892.

2 S. Han, X. Yang, X. Hu, Y. Wang and F. Wu, *Polym. Degrad. Stabil.*, 2023, **217**, 110518.

3 W. Luo, T. Wang, X. Gou, J. Luo, W. L. An, Z. C. Fu, J. N. Deng, H. B. Zhao and M. J. Chen, *ACS Mater. Lett.*, 2024, **6**, 5418-5428.

4 W. F. Tang, G. Q. Liang, L. Wang, Y. Yuan, W. Dessie, F. Liu, Z. D. Qin, Y. Wang, A. G. Xiao and X. D. Jin, *J. Clean. Prod.*, 2023, **394**, 136371.

5 J. F. Feng, T. Wang, C. X. Xu, X. Gou, L. He, Z. C. Fu, J. N. Deng, W. L. An, N. Jiang and H. B. Zhao, *ACS Mater. Lett.*, 2025, **7**, 2031-2040.

6 S. H. Yin, Y. R. Du, X. D. Liang, Y. H. Xie, D. L. Xie and Y. Mei, *Appl. Surf. Sci.*, 2023, **637**, 157961.

7 H. P. Fang, J. T. Wang, Y. Deng, W. J. Hu, Y. M. Li and D. Y. Wang, *Polym. Degrad. Stabil.*, 2025, **242**, 111726.

8 Y. B. Huang, S. H. Jiang, R. C. Liang, Z. W. Liao and G. X. You, *Compos. Part A Appl. Sci. Manuf.*, 2019, **125**, 105534.

9 Y. F. Gao, W. J. Tang, R. Wang, M. F. Guan, J. J. Sun, H. M. Long, X. Y. Liu, R. Cai and G. Tang, *Int. J. Biol. Macromol.*, 2025, 144623.

10 X. Li, Y. Xu, X. Y. An, L. Gong, R. Wang and Z. M. Liu, *Int. J. Biol. Macromol.*, 2025, **304**, 140947.

11 X. Zhang, Q. Guan, S. Ding, Z. Wang and H. Xie, *Construct. Build. Mater.*, 2025, **479**, 141517.

12 O. Su and Y. Wang, *Process Saf. Environ. Prot.*, 2025, **202**, 107813.

13 X. Zhang, Q. H. Guan, S. Ding, Z. Wang and H. Xie, *Case Stud. Therm. Eng.*, 2025, **69**, 106039.

14 K. Selvaraj, H. F. He, M. E. Spontón, N. Sun, H. L. Ding, Y. Yuan, C. S. Wang, L. Liu, Y. X. Yi and B. Yu, *Polym. Degrad. Stabil.*, 2025, **243**, 111745.

15 X. Zhang, R. Han, Q. H. Guan, Y. Zhang, Z. Wang and H. Xie, *Int. J. Polym. Anal. Charact.*, 2025, **30**, 271-286.

16 L. C. Sun, Y. J. Guo, R. X. Ou, J. W. Xu, F. Gao, Q. Z. Meng, S. L. Chen, C. G. Guo, Q. Fan and Q. W. Wang, *Adv. Funct. Mater.*, 2024, **34**, 2405424.

17 M. S. Fidan and M. Ertaş, *BioResources*, 2020, **15**, 6080.

18 M. Zemła, A. Prociak and S. Michałowski, *Polymers*, 2021, **14**, 102.

19 P. Acuña, J. Zhang, G. Z. Yin, X. Q. Liu and D. Y. Wang, *J. Mater. Sci.*, 2021, **56**, 2684-2701.

20 P. L. De Hoyos-Martinez, S. B. Mendez, E. C. Martinez, D. Y. Wang and J. Labidi, *Polymers*, 2024, **16**, 258.

21 T. M. Nguyen-Ha, T. B. Nguyen, T. A. Nguyen, L. H. Pham, D. H. Nguyen, D. M. Nguyen, D. Hoang, E. Oh and J. Suhr, *Chem. Eng. J.*, 2023, **474**, 145585.

22 G. Y. Zhang, X. Q. Lin, Q. Q. Zhang, K. S. Jiang, W. S. Chen and D. Z. Han, *RSC Adv.*, 2020, **10**, 32156-32161.

23 E. Akdogan, M. Erdem, E. Kaynak and M. E. Ureyen, *Iran. Polym. J.*, 2024, **33**, 381-394.

24 X. L. Chen, F. R. Zeng, W. X. Li, L. Zhang, C. Deng, Y. Tan, M. J. Chen, S. C. Huang, B. W. Liu and Y. Z. Wang, *J. Mater. Sci. Technol.*, 2023, **162**, 179-188.

25 J. T. Cao, N. L. Shen, C. S. Yan, Y. Zhao, C. B. Yu, S. He, Z. F. Huang and W. H. Rao, *Construct. Build. Mater.*, 2025, **500**, 144142.

26 N. Yu, T. Wang, C. X. Xu, X. Gou, Y. J. Zhan, W. An, Z. C. Fu, J. N. Deng, H. B. Zhao and M.

J. Chen, *Chem. Eng. J.*, 2025, **503**, 158514.